Available online at www.sciencedirect.com
SCIENCE DIRECT®
Icarus 167 (2004) 80–88
ICARUS
www.elsevier.com/locate/icarus

Solar wind interactions with Comet 19P/Borrelly

D.T. Young,[a,*] F.J. Crary,[b,1] J.E. Nordholt,[c] F. Bagenal,[d] D. Boice,[a] J.L. Burch,[a] A. Eviatar,[e] R. Goldstein,[a] J.J. Hanley,[a] D.J. Lawrence,[c] D.J. McComas,[a] R. Meier,[f] D. Reisenfeld,[c] K. Sauer,[g] and R.C. Wiens [c]

[a] *Southwest Research Institute, P.O. Drawer 28510, San Antonio, TX, 78228-0510, USA*
[b] *The University of Michigan, Department of Atmospheric, Oceanic and Space Sciences, Ann Arbor, MI 48109, USA*
[c] *Los Alamos National Laboratory, Los Alamos, NM 87544, USA*
[d] *University of Colorado, Laboratory for Atmospheric and Space Physics, Boulder, CO 80309-0392, USA*
[e] *Tel Aviv University, Department. of Geophysics and Planetary Sciences, Ramat Aviv, Israel*
[f] *University of Hawaii, Institute of Astronomy, Honolulu, HI 96822, USA*
[g] *Max Planck Institute for Aeronomy, D-3411 Katlenburg-Lindau, Germany*

Received 6 December 2002; revised 12 September 2003

Abstract

The Plasma Experiment for Planetary Exploration (PEPE) made detailed observations of the plasma environment of Comet 19P/Borrelly during the Deep Space 1 (DS1) flyby on September 22, 2001. Several distinct regions and boundaries have been identified on both inbound and outbound trajectories, including an upstream region of decelerated solar wind plasma and cometary ion pickup, the cometary bow shock, a sheath of heated and mixed solar wind and cometary ions, and a collisional inner coma dominated by cometary ions. All of these features were significantly offset to the north of the nucleus–Sun line, suggesting that the coma itself produces this offset, possibly because of well-collimated large dayside jets directed 8°–10° northward from the nucleus as observed by the DS1 MICAS camera. The maximum observed ion density was 1640 ion/cm^3 at a distance of 2650 km from the nucleus while the flow speed dropped from 360 km/s in the solar wind to 8 km/s at closest approach. Preliminary analysis of PEPE mass spectra suggest that the ratio of CO^+/H_2O^+ is lower than that observed with Giotto at 1P/Halley.

Keywords: Comets, dynamics; Comets, composition; Solar wind

1. Introduction

Previous in situ measurements of the plasma environments of cometary comae have been obtained during encounters with Comets 21P/Giacobini–Zinner (GZ; encounter on 9/11/85 at 1.03 AU; $Q = 2 \times 10^{28}$ molecules/s), 1P/Halley (five encounters took place from 3/6/86 to 3/14/86 at 0.79 to 0.89 AU, respectively; $Q = 1 \times 10^{30}$ to 7×10^{29} molecules/s, respectively); and 26P/Grigg–Skjellerup (GS; encounter on 7/10/92 at 1.01 AU; $Q = 7 \times 10^{27}$ molecules/s). These data, combined with theory and modeling, have established the current understanding of coma morphology and dynamics. What has emerged is that a weak bow shock or compressional wave forms in supersonic but mass-loaded solar wind plasma as it approaches the inner coma. Inside the shock, there are several distinct collisional and magnetic boundaries (for reviews see Mendis et al., 1986; Ip and Axford, 1990; Cravens, 1991; Klummer, 1991; Neubauer, 1991; Schmidt and Wegmann, 1991). In addition to standard coma features, there are also significant differences among the observations that can be attributed to several factors. For one thing, total nucleus gas and dust production rates, as well as solar wind parameters, have been different during each encounter. In addition, nucleus properties such as spin rate, spin axis orientation, and spatial distribution of gas and dust production can contribute to variations in coma morphology (Sekanina, 1991; Huebner et al., 1991). Finally, the nature of the solar wind-comet interaction is very dynamic, making it difficult to

* Corresponding author.
E-mail address: dyoung@swri.edu (D.T. Young).
[1] Present address: Southwest Research Institute, USA.

0019-1035/$ – see front matter
doi:10.1016/j.icarus.2003.09.011

consistently identify characteristic boundaries and features during a single, rapid spacecraft traversal of the coma.

In this paper we present observations of the coma of comet Borrelly, which show a number of morphological aspects not reported previously, but that may be characteristic of active comets having highly non-uniform gas production rates across the surface of the nucleus, which appears to be the case at Borrelly (Soderblom et al., 2002).

Cometary gases, mainly water, expand outward from the comet nucleus at speeds $V_n \sim 1$ km/s. Far from the nucleus, solar UV photons ionize these molecules on characteristic time scales of $10^4 \sim 1.6 \times 10^6$ s, corresponding on average to $\sim 10^5$ km from the nucleus, at the heliocentric distance of Borrelly, (1.36 AU; nearer the nucleus other processes such as charge exchange become important). New ions are created at rest with respect to the solar wind in the spacecraft frame of reference. They are accelerated ("picked up") by the solar wind electric field $E_{\rm sw} = -U_{\rm sw} \times B_{\rm sw}$, where $U_{\rm sw}$ is the solar wind velocity in m/s and $B_{\rm sw}$ the vector magnetic field in tesla. The maximum pickup energy of an ion of mass M (in AMU) is given by $E_{\rm max} = 0.021M(V_s \sin\theta)^2$, where V_s is the solar wind velocity in km/s, and θ is the angle between solar wind flow velocity and the local magnetic field direction. Thus the energy of singly-charged pickup ions varies from zero to ~ 4 keV/nucleon in the spacecraft frame. One important effect of the pickup process is that the addition of heavy ions initially at rest reduces the speed of the solar wind. The other is that intense plasma waves are generated in the process of ion pickup, causing wave–particle interactions that couple the collisionless solar wind and cometary plasmas to each other.

Pickup cometary ions are initially cold and nearly stationary relative to the neutral gas of the comet, but in the solar wind frame of reference appear to be hot, creating a narrow ring-beam distribution in that frame. Such a distribution is unstable, leading to the generation and growth of low-frequency waves. Wave-field fluctuations are large enough to cause ion pitch angle diffusion and scattering (the dominant process depending on the intensity of the fluctuations), instigate fluid instabilities, and lead to second-order Fermi acceleration of ions to hundreds of keV. (Papers by Gary et al., 1986; Ip, 1988; Johnstone et al., 1991; Yoon and Wu, 1991; Coates et al., 1993; Huddleston et al., 1994; Tsurutani, 1991; Tsurutani et al., 1995, summarize various aspects of these processes.) Depending on gas production rate and solar wind conditions, a bow shock (Balsiger et al., 1986; Johnstone et al., 1986; Balsiger, 1989; Schmidt et al., 1993) or bow wave (Thomsen et al., 1986) may form in the mass-loaded solar wind, slowing the solar wind further, diverting plasma flow around the dense inner coma, and heating the streaming plasma. In addition, an inner shock or compressional wave may form (Gombosi, 1987). As the flow penetrates deeper into the coma, neutral gas density becomes sufficiently high that ion-neutral particle collisions begin to dominate fluid and chemical characteristics of the flow (Gombosi, 1987; Cravens, 1991; Reme, 1991; Huebner et al., 1991; Haberli et al., 1995, 1997). The region where this occurs is termed the collisionopause (several such boundaries could be defined depending on the collisional process of interest, see Gombosi (1987) and Cravens (1991)). Along the central axis of the comet–Sun line, solar wind flow eventually drops to a few km/s, the flow nears stagnation, and slips around a flow boundary called the cometopause (Cravens, 1991). Since the slowing plasma flow carries magnetic field with it, magnetic flux piles at this boundary, creating a diamagnetic cavity inside.

Over the past 16 years a total of seven spacecraft, including DS1, have made *in situ* observations of the near-perihelion plasma environments of four different comets: 21P/Giacobini–Zinner, 1P/Halley, 26P/Grigg–Skjellerup, and now 19P/Borrelly. Gas production rates of the four comets varied over two orders-of-magnitude at the time of observation. Comet GS, visited by the Giotto spacecraft in July 1992, had a relatively low production rate of 7.5×10^{27} mol/s but was a surprisingly rich source of plasma physical phenomena nonetheless (Coates et al., 1993; Johnstone et al., 1993; Schmidt et al., 1993). The Borrelly production rate during DS1 encounter was roughly four times higher at 3.5×10^{28} mol/s (Weaver et al., 2003; Schleicher et al., 2003; Szabó et al., 2002), and roughly equal to that of Comet Giacobini–Zinner (GZ) during the International Cometary Explorer (ICE) observations in September 1985 (Cravens, 1991). Comet Halley's production rate was 7 to 10×10^{29} mol/s during the Giotto, Vega 1 and 2, Suisei, and Sakigake encounters in March 1986 (Tsurutani et al., 1995), or roughly 20 to 30 times that of Borrelly. ICE observations were made 7800 km downstream from the nucleus of GZ.

At GZ, a compressional bow wave and turbulent magnetosheath region were observed, but there was no evidence for a shock. However, plasma instabilities and strong MHD turbulence were very much in evidence, a rather surprising finding at the time (Gary et al., 1986; Bame et al., 1986; Ip, 1988). Morphologically, the cometary ion tail of GZ was found to be closely centered on the nucleus–Sun axis to within ~ 500 km (Bame et al., 1986; Mendis et al., 1986). The two Vega spacecraft passed inside 9000 km upstream of Halley's nucleus while Giotto came within 600 km. A review of these observations by Balsiger (1989) identified a weak upstream bow shock $\sim 1.1 \times 10^6$ km from the nucleus (measured along the spacecraft trajectory, i.e., corresponding to a subsolar distance of $\sim 0.55 \times 10^6$ km). At the shock there is a sudden drop in bulk flow velocity, and an increase in the density of both protons and cometary ions. At $\sim 8 \times 10^4$ km from the Halley nucleus, a collisional boundary was observed in which magnetic field intensity increased, the density of protons and He^{2+} decreased, the density of cometary ions increased, and the inward flow of plasma stagnated (Balsiger et al., 1986; Shelley et al., 1987; Haberli et al., 1995).

Inside the collisionopause (roughly $\sim 10^5$ km from the nucleus at Halley) two- and even three-body collisions begin

to occur, setting off a wide range of complex physical and chemical processes including charge transfer, ion-neutral collisions and electron impact ionization (Ip and Axford, 1990; Cravens, 1991; Haberli et al., 1995, 1997). Charge transfer reduces the ionized component of the solar wind and is greatest where the ion mean free path ($\sim R^3$), begins to decrease rapidly (Gombosi, 1987). Ion-neutral collisions lead to momentum exchange (Gombosi, 1987; Haberli et al., 1995, 1997) and formation of the collisionopause roughly at the point where the solar wind mean free path is comparable to the distance to the nucleus (Ip and Axford, 1990; Cravens, 1991). At Borrelly, R_C is estimated to be inside the DS1 closest approach distance. Depending on the balance between pressure generated by gas outflow from the nucleus and that caused by the inflow of plasma and magnetic field, a sharply demarcated magnetic cavity may form. Although observed by spacecraft at Halley and possibly downstream of the nucleus at GZ, the magnetic boundary at Borrelly was most likely located within a few hundred km of the nucleus, well inside the DS1 closest approach distance of 2171 km.

2. Instrumentation

The PEPE instrument consists of separate ion and electron spectrometers that simultaneously measure the energy and angular distributions of electron and ion fluxes, and the composition of ions (Young et al., 2003). PEPE measures electron and ion energy/charge (E/q) from 8 to 33,000 eV/q with a resolution ($\Delta E/E$) of 0.07. Directions of arrival are measured over a field-of-view covering $\pm 45^\circ$ in elevation by 360° in azimuth or roughly 70% of the unit sphere. The electron FOV is divided into 256 pixels each $5^\circ \times 22.5^\circ$ whereas the ion FOV is divided into 256 pixels varying from $5^\circ \times 5^\circ$ to $5^\circ \times 45^\circ$ opposite the solar wind direction. During the flyby PEPE was oriented such that the solar wind and comet velocity vectors were within the FOV, and were in or near the finer resolution ion pixels.

Energy and angle parameters are sampled by fixing the instrument on an energy step, scanning the elevation by $\pm 45^\circ$ and then advancing to the next energy step. Each scan of angle requires 0.51 s, yielding a complete scan in angle and energy once every 65.5 s. At each ion energy and angle, the time-of-flight (TOF) mass spectrometer builds up an ion spectrum from which mass/charge (M/q) is derived over the range 1 to 150 amu/q with a mass resolution $M/\Delta M \approx 20$ at 10% of peak height (based on pre-encounter measurements of solar wind He^{++}). Telemetry restrictions limit the data returned to Earth to energy resolution of 0.15, angular resolution of $20^\circ \times 90^\circ$ for electrons and $11^\circ \times 11^\circ$ to $11^\circ \times 90^\circ$ for ions. Composition data are returned as time-of-flight spectra, summed over all energies and angles, and as energy spectra of selected ion species. In this paper we report primarily on ion observations. Electron data require further analysis to remove the effects of spacecraft photoelectrons and spacecraft potential.

The PEPE time-of-flight unit consists of a ceramic cylinder resistively coated on the inside surface. The resistivity of the cylinder surface is carefully distributed so that when biased by equal negative and positive at the entrance end and the detector end, a linear electric field (LEF) is created (McComas and Nordholt, 1990). The field is oriented to reflect incoming positively charged ions. In operation, the negative bias accelerates ions exiting the energy analyzer into thin (~ 1 microgram/cm^2) carbon foils located at the LEF entrance. As a result of collisions in the foils, incident ions scatter, lose energy, and change charge state, exiting the foil as neutral atoms or as ions of either positive or negative charge depending on ion species and total energy entering the foil. Upon exiting the foils, ions (or neutrals) knock out secondary electrons, which are collected on a detector whose signal starts the time-of-flight (TOF) measurement. In the case of oxygen, for example, the negative ion yield is large (Funsten et al., 1993). Positive ions emerging from the foil with energies < 13 keV are reflected by the LEF in such a way that their times of flight are independent of exit energy (McComas and Nordholt, 1990; McComas et al., 1998). All other ions and neutrals travel directly to the detector (Young et al., 2003). In the PEPE design, a single detector is used in contrast to two employed in a similar spectrometer on a similar instrument flown on the Cassini mission (McComas et al., 1998). The PEPE TOF design permits all three exiting charge states from the foil to be detected in the same TOF spectrum, facilitating deconvolution. Further, the electric field accelerates negative ions, producing a separate peak at shorter times of flight than that of the neutrals and LEF-reflected positive ions. During flight operations, damage to the PEPE high voltage cylinder reduced mass resolution performance.

3. Observations

DS1 flew through the Borrelly coma on the sunward side of the nucleus, moving from north to south relative to the plane of the ecliptic at a speed of 16.5 km/s relative to the nucleus. The encounter geometry placed the angle of the DS1 trajectory at 8° relative to the ecliptic and approximately perpendicular to the Sun–nucleus line. The DS1 velocity corresponded to 1080 km per instrument measurement cycle of 65.5 seconds. Closest approach was at a distance of 2171 km from the nucleus at 22:29:33 UTC, spacecraft event time. During the DS1 encounter period from -10.5 hr before CA to $+7.5$ hr after, DS1 was alternately pointed towards Earth, a guide star located near Borrelly on the sky as seen from DS1, and the Borrelly nucleus (Rayman, 2002). (This paper uses decimal hours relative to CA so that 12:29:33 UTC on September 22 corresponds to -10.5 hr, CA = 0.0 hr, etc.) As seen from DS1, the spacecraft approached the nucleus from above, i.e., from north of the ecliptic plane, at an asymptotic phase angle of 90°.

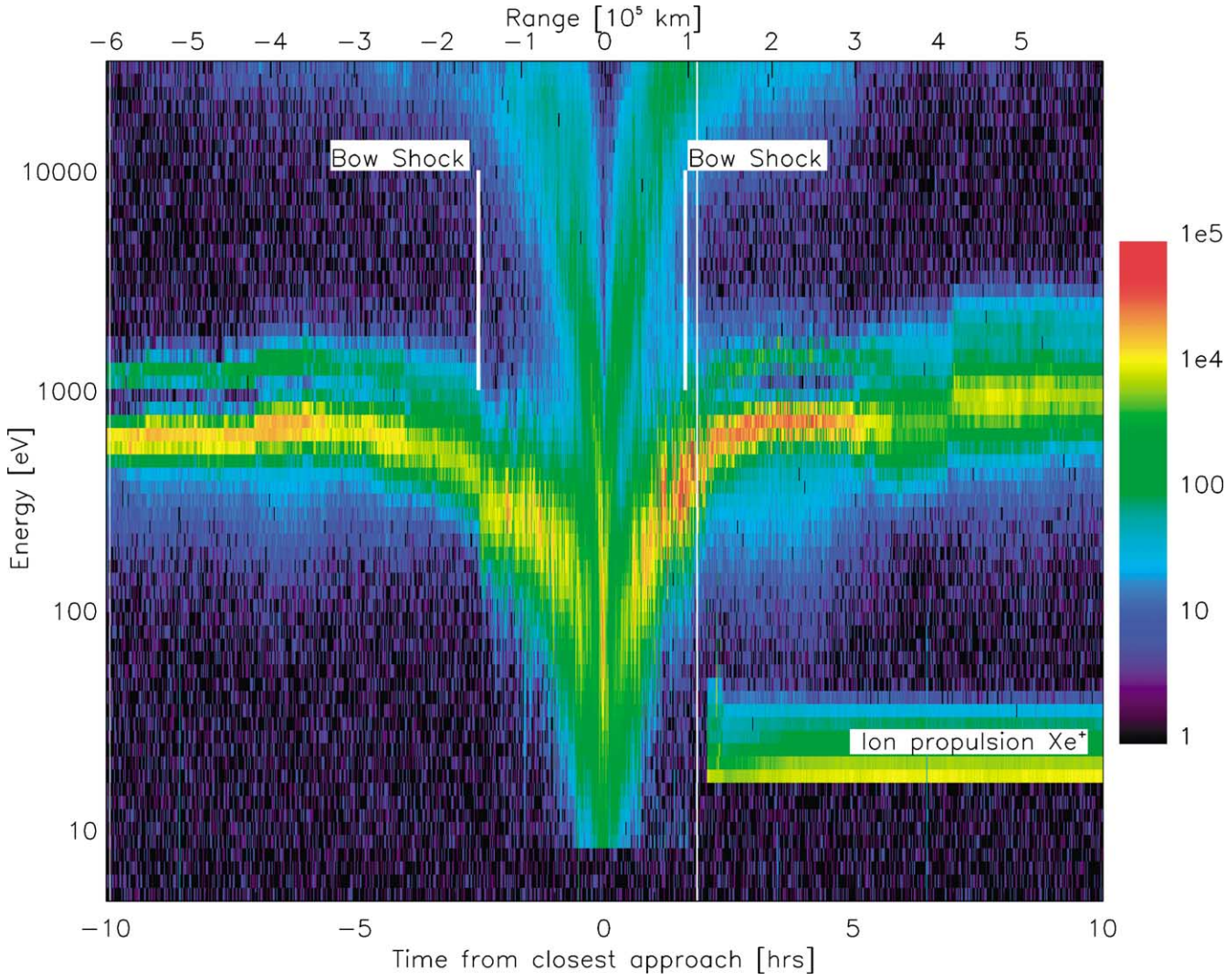

Fig. 1. PEPE total ion counting rate (coded as color) plotted as a function of ion energy in units of eV (ordinate) and time in hours (abscissa). Time extends from 10.5 hours (6.3×10^5 km) before closest approach to 13.5 hours (8.1×10^5 km) after. Closest approach occurred at 22:29:33 UTC. At 00:31:30 UTC on 23 September the DS1 ion propulsion system was started, causing the burst of first hydrazine and then xenon ions to be observed by PEPE. (All times are spacecraft event time.) The ion counting rate, C, is proportional to differential number flux, J_E, through the relation $C = J(E)EG$, where $J(E)$ is differential ion flux in units of ions $\mathrm{cm}^{-2}\,\mathrm{s}^{-1}\,\mathrm{sr}^{-1}\,\mathrm{eV}^{-1}$ and G is the instrument sensitivity.

Figure 1 shows PEPE ion data in an energy-time spectrogram format covering the entire encounter period. In this format color codes for ion flux intensity and all ion species regardless of mass are included. Solar wind He^{++} is the upper trace to the far left in the figure, while the lower, more intense trace, is H^+. Although barely visible initially in the figure, heavy ions can be seen from $\sim$ 0700 UT onwards at the top of the figure, indicating their high pickup energy. Features in Fig. 1 are similar to those in spectrograms shown in Johnstone et al. (1986) and Coates et al. (1993). Total ion density measured during the Borrelly encounter is plotted in Fig. 2 and flow velocity in Fig. 3.

The density and velocity of the plasma can be calculated by taking statistical moments of the PEPE energy-angle spectra. This commonly used technique, however, requires knowledge of the plasma composition to give accurate results. Rigorously, the values obtained from statistical moments are $\langle (q/m)^{1/2} \rangle n$ and $n\underline{\mathbf{v}}$, where n is the density, $\underline{\mathbf{v}}$ the velocity, and $\langle (q/m)^{1/2} \rangle$ the density-weighted mean of the square root of the ions' charge to mass ratio. An assumed or measured composition is therefore required to determine ion density and velocity. Our analysis of the PEPE data is based on the observed energy spectra of the dominant ion species, specifically those of H^+(TOF bins 47-88) and water group ions (TOF bins 151-458). Because the time of flight bins were summed over angle on the spacecraft (making them less sensitive than energy-angle spectra integrated over all species), and their absolute calibration is not as well known as the total-ion calibration, binned TOF data are not used to calculate moments. Instead, the energy spectra from selected TOF bins are used to calculate only the relative abundance of H^+ and water group ions. From the shapes of the TOF

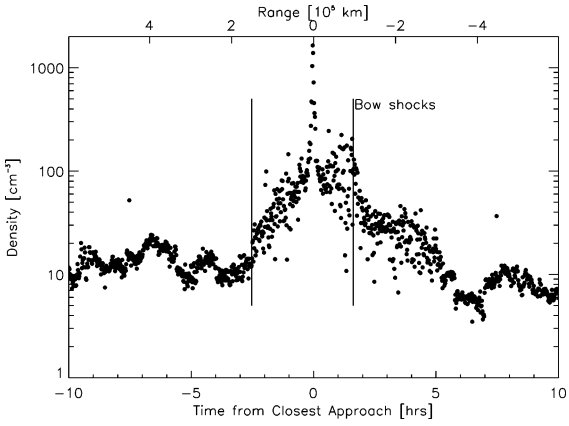

Fig. 2. Total ion density measured by PEPE on September 22–23, 2001. Closest approach occurred at 22:29:33. Density was calculated by taking statistical moments of the data (see text). The variations in density from spectrum to spectrum suggest the presence of strong plasma waves.

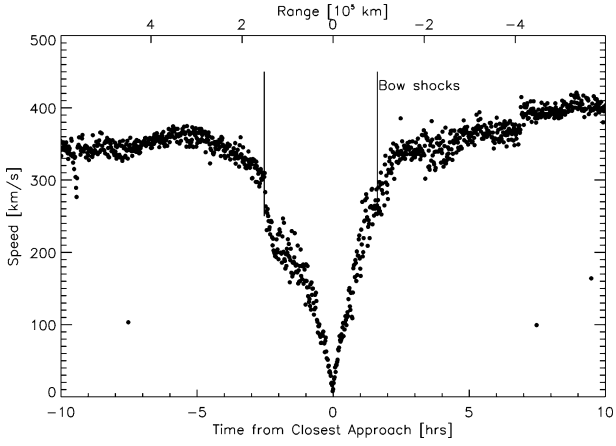

Fig. 3. Ion velocity measured by PEPE on September 22–23, 2001. A weak inbound bow shock is visible near −3 hours. The stronger shock at +7 hours is interplanetary and unrelated to the comet.

spectra, we assume these are the dominant species, and that the water group ions have an average mass of 17 AMU. These data, combined with the moments of the energy-angle spectra, are then used to determine plasma density and flow velocity.

Beginning with PEPE coverage at CA -6.3×10^5 km, the solar wind density and velocity are 10–20 cm^{-3} and 340 km/s, the latter corresponding to a flow energy of 604 eV. Assuming that pickup ions are on average mass 17 at this distance and $V_{sw} = 340$ km/s, then E_{max} is approximately 41 keV. The solar wind velocity, before and after the encounter, was essentially unchanged and the density did not change substantially. This lends support to our conclusion that any large change in plasma parameters must be caused by solar wind interactions with the coma, and not by the solar wind acting alone (Mendis et al., 1986; Huddleston et al., 1994). A small interplanetary shock occurred on September 23 at +06.92 hr (Figs. 1–3), when DS1 was $+4.15 \times 10^5$ km from the nucleus and well outside the

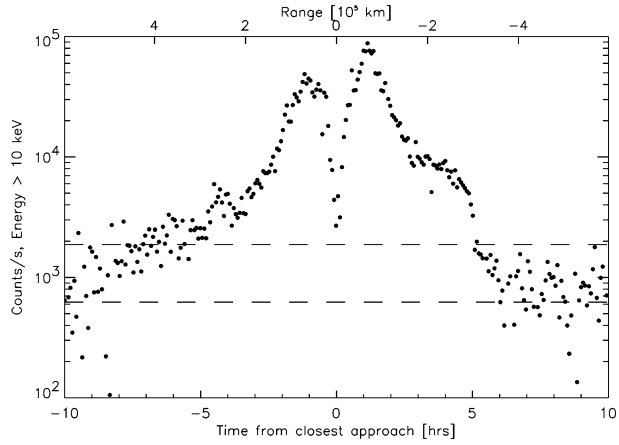

Fig. 4. Observed count rate of ions with energies above 10 keV. The dashed lines show the 1 and 3 sigma statistical uncertainty. Cometary energetic ions were observed between −7 and +5 hours of closest approach. The drop in the count rates near closest approach results from the slowing of the flow and the mean particle energy dropping below the 10 keV threshold of this figure.

cometary shock. It therefore should have no bearing on results reported here.

At −9.33 hr and -5.88×10^5 km from Borrelly, DS1 completed a turn to Earth-pointing attitude from its thrust attitude. This orientation centered the PEPE FOV on the solar wind ram direction for the first time during the encounter sequence. In this more favorable viewing attitude, pickup ions above 10 keV/e (Fig. 4) first began to appear.

The initial mean pickup ion energy was above the PEPE limit of 33 keV, consistent with expectations for the pickup process far from the comet. Similar fluxes of 10 to 33 keV ions were observed until $+3.6 \times 10^5$ km on the outbound leg (Table 1). Farther along the inbound leg, at -4.26×10^5 km (−7.08 hr) there is a jump in ion number flux (nv) by a factor ∼ 2.5, most likely attributable to a compression of the upstream solar wind.

The solar wind speed reached a maximum of ∼ 370 km/s (Fig. 3) and then began to slow noticeably at -2.1×10^5 km (−3.5 hr) from the nucleus. Although the pickup ion number density was below 1% of the proton density, slowing of the flow indicates that pickup ions accounted for ∼ 10% of the mass density at this distance. A similar degree of slowing on the outbound trajectory occurred $+1.2 \times 10^5$ km from the nucleus. Slowing and heating of the solar wind continued for the next hour until the cometary bow shock was encountered at -1.52×10^5 km (−2.53 hr) from the nucleus (Fig. 3). At the shock there is a moderate but sharp decrease in solar wind flow velocity from 275 to 240 km/s accompanied by an increase in proton and He^{2+} heating (Fig. 1) and the rate at which ions > 10 keV/e are added to the flow (Fig. 4). These data are interpreted as evidence of ion heating in the turbulent cometosheath behind the shock, even as the bulk plasma velocity decreases (Johnstone et al., 1991; Coates et al., 1993). The outbound shock at $+9.6 \times 10^4$ km is less distinct. Although density and velocity contrasts across

Table 1
Summary of estimated cometary plasma boundaries relative to comet–Sun line

Boundary	Inbound		Outbound		Average subsolar	Displacement
	Time [hr]	Distance [10^3 km]	Time [hr]	Distance [10^3 km]	distance[a] [10^3 km]	ratio (D)
Pickup ions observed	−9.33	588	+6.00	360	237	0.48
10% solar wind slowing	−3.50	210	+2.00	120	83	0.55
Bow shock	−2.53	152	+1.62	96	62	0.45
Change in ion flux < 10 keV	−1.25	75	+1.08	65	35	0.14
Cometopause	−0.25	15.1	+0.15	8.6	5.9	0.55
Center of ion density	−0.03	1.5				

[a] Assumes boundary has a parabolic shape.

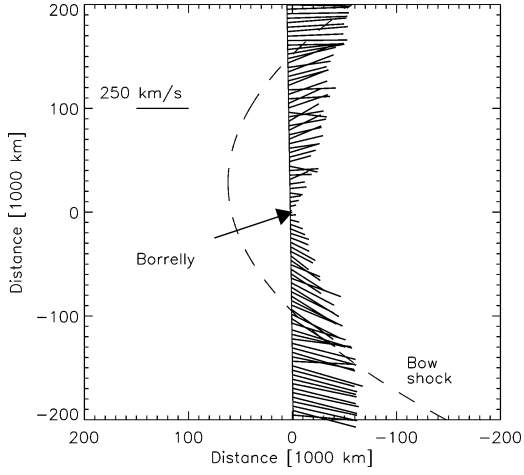

Fig. 5. DS1 trajectory with measured ion velocity vectors. Lines starting at the spacecraft's position point in the direction of the flow, and their length indicates the flow speed. In this figure, the $+X$-axis points to the Sun and the spacecraft's trajectory relative to the nucleus is in the X–Y plane. This causes the $+Y$ to point near the north ecliptic pole.

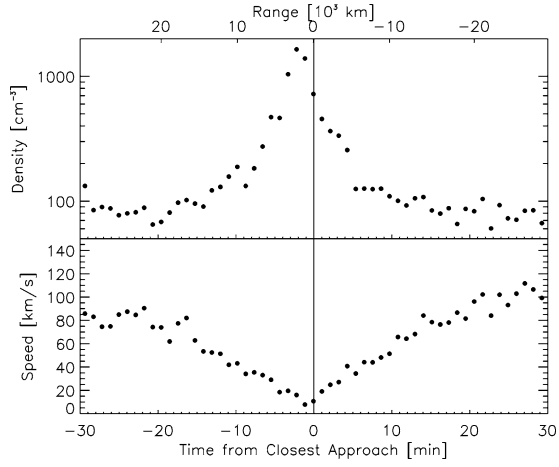

Fig. 6. PEPE measurements of total ion density and speed are shown on an expanded scale near closest approach. The ion density peaks at between 1 to 2 minutes, or ∼ 1500 km, before closest approach. The flow speed may also be asymmetric about closest approach but this is not as obvious since the profile is broader than that of the density.

the outbound shock are smaller than inbound, the shock coincides with sharp changes in proton temperature and the apparent level of plasma turbulence (Fig. 1).

Total ion flow (i.e., all species included) in the cometosheath region clearly follows a pattern directed away from the comet (Fig. 5) as the nucleus–Sun line is approached.

This is consistent with MHD models of solar wind flow around comets (Schmidt et al., 1993). If the plasma boundaries at Borrelly are parabolic in shape (Mendis et al., 1986) and flare at a ratio of 2 : 1 between the flank, where DS1 is located, and the subsolar point, then a rough estimate of the subsolar distance to the Borrelly bowshock is $\sim 6.2 \times 10^4$ km, roughly twice that expected from theoretical estimates (Ipavich et al., 1986; Cravens, 1991) scaled to Borrelly conditions.

Inside -7.5×10^4 km from CA (-1.25 hr), the number of pickup ions above 10 keV starts to decrease rapidly (Figs. 1 and 4) as their mean energy falls below 10 keV and the bulk of pickup water-group ions enters the PEPE energy range. No corresponding change seems to occur in any of the other ion parameters. On the outbound leg this boundary occurs at $+6.5 \times 10^4$ km ($+1.08$ hr).

Within 10,000 km of the nucleus, the ion density increases rapidly, reaching a peak of 1640 cm^{-3} approximately 1500 km prior to closest approach (Fig. 6).

During this period, the water group abundance increased relative to total plasma density. Between $-15{,}200$ and $+8600$ km, the water group ion abundance exceeded 50% and peaked at over 90%, approximately 1500 km before closest approach. The near-nucleus perturbations to ion speed have a broader profile, with a minimum speed of 8 km/s roughly centered on closest approach. This resembles the cometopause region observed at Halley, which occurs when collisional processes such as charge transfer and Coulomb scattering become important factors in slowing the flow of mass loaded solar wind (Gombosi, 1987; Cravens, 1991; Haberli et al., 1995). Collisionless momentum coupling via wave-particle interactions between protons and heavy ions may also contribute to slowing (Sauer et al., 1994). A simple analytical mass-loading model can be used to estimate the location of the subsolar cometopause. Following Gombosi (1987), $R_{\rm com} = ((U_{\rm th}/U_{\rm sw}) R_{\rm s} R_{\rm o})^{1/2}$, where $U_{\rm th}$ is the ion thermal velocity, $R_{\rm s}$ is the sub-solar shock distance, and $R_{\rm o}$ the charge exchange scale length. From PEPE observations we estimate approximately $U_{\rm th} \sim$

$U_{sw} \sim 40$ km/s (Fig. 6), $R_s \sim 7.2 \times 10^4$ km, and $R_o = \sigma_{ct} Q_n / 4\pi V_n \sim 4.3 \times 10^2$ km (taking $\sigma_{ct} \sim 3 \times 10^{-15}$ cm^2). This gives $R_{com} = 5560$ km. The average of observed inbound and outbound cometopause crossings (Table 1) is 11,900 km, at approximately 70° from the nucleus–Sun line. If this boundary has a parabolic shape, it could be roughly a factor of two closer to the nucleus in the sub-solar direction, in agreement with theory.

As noted previously, and summarized in Table 1, every major plasma boundary observed on both inbound and outbound legs of the encounter is asymmetric to some degree about the nucleus–Sun line and closest approach point. The asymmetry corresponds to displacements to the north of a plane containing Borrelly and the Sun and parallel to the ecliptic plane. Boundary distances that are very different on the inbound and outbound legs are those where pickup ions < 33 keV begin to be observed, where the solar wind slowing starts, and where the cometopause is found. The drop in energetic pickup ion fluxes is less asymmetric, but is still displaced northwards (Table 1), as is the peak in total ion density near closest approach (Fig. 6).

The relative displacements of these boundaries can be quantified simply by defining $D = 2(y_1 - y_2)/(y_1 + y_2)$, where y_1 and y_2 correspond to boundary locations along the inbound and outbound trajectories, respectively (since the encounter distance $D_E \ll D$ for all boundaries discussed here, we can treat y_1 and y_2 as straight, unsigned lines). Although we are not in a position to put strong error limits on these findings, they clearly indicate a large and consistent asymmetry in the comet coma that does not appear to have been observed before. The most complete sets of plasma data taken on both inbound and outbound legs during previous encounters are those of Bame et al. (1986) at GZ, Johnstone et al. (1986) and Balsiger et al. (1986) at Halley, and Coates et al. (1993) at GS. If we use the positions of the five plasma boundaries identified by Bame et al. and, for the sake of comparison, calculate the average value of D at GZ, we obtain $D = 0.14$, compared to 0.43 for the Borrelly data presented here. The average of the three transition boundaries identified by Johnstone et al. (1986) at Halley was $D = 0.23$. There is no direct way to compare these boundaries, but it is worth noting that at each comet they are all found consistently on the same side of the nucleus–Sun line. Some of this displacement is caused by magnetic field line draping.

The PEPE time-of-flight (TOF) mass spectra indicate the presence of He^+ as well as the expected protons, solar wind alpha particles and cometary water group ions. Figure 7 shows a TOF spectrum averaged over ± 11.5 minutes ($\pm 11{,}500$ km) around closest approach. This time interval corresponds roughly to the region inside what we identify as the cometopause (-15 minutes to $+9$ minutes around CA, see Table 1) while also taking into account the duration of the PEPE TOF measurement cycle.

We show here the expected location of neutral and negative TOF peaks from incident water group, CO^+ and CO_2^+ ions. The main water group ions observed with PEPE are

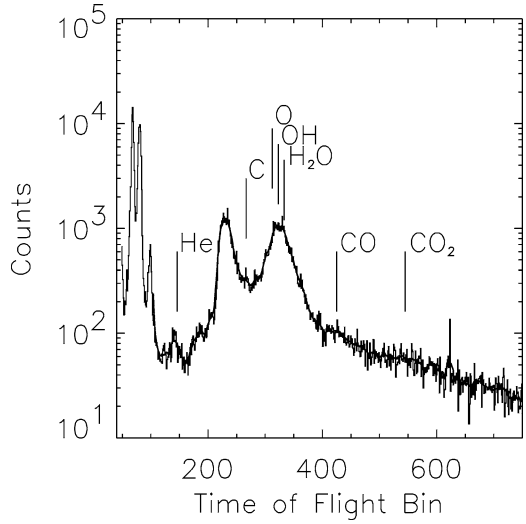

Fig. 7. Mass spectrum averaged over $\pm 11{,}500$ km around closest approach distance. Water group ions and their daughter ions dominate the composition. He^+ ions, charge exchanged from He^{++} in the solar wind, are also present. The two sharp peaks at small times-of-flight are both due to incident H^+ from the solar wind and comet. The large peak near TOF bin 230 is produced by oxygen, which exits the instrument's carbon foil with a negative charge causing it to be accelerated (see text).

OH^+ and H_2O^+, which coincide with the two main broad peaks in the figure, rather than H_3O^+, which was the dominant species observed by Giotto at Halley (Balsiger et al., 1986; Krankowsky et al., 1986; Eberhardt et al., 1987; Haberli et al., 1995). We attribute this primarily to the trajectory of DS1, which very likely did not penetrate deeply enough into the inner coma to observe large amounts of H_3O^+. Chemical modeling is required to determine whether the gas production rate of Borrelly was sufficient to produce H_3O^+, since the appropriate reactions are a strong function of neutral density. The He^+ seen in the spectrum in Fig. 7 is produced by charge transfer reactions between cometary neutrals and solar wind alpha particles. Similar charge transfer reactions, involving solar wind heavy ions, are associated with the production of cometary X-rays (Cravens, 1997, 2002). The maximum He^+ abundance occurred approximately 2000 km before closest approach, where the $[He^+]/([He^+] + [He^{++}])$ ratio was 0.4. This ratio is a measure of the neutral density integrated along a streamline from the Sun to the spacecraft, which is approximately equal to the neutral column density between the Sun and spacecraft. A symmetric Haser model (Haser, 1957) using an outflow velocity of 1 km/s, an ionization lifetime of 1.6×10^5 s, and rates for helium reactions taken from Greenwood et al. (2000) would require a total water production rate over 2×10^{29} s^{-1} to produce a ratio of 0.4 (Shelley et al., 1987). This is roughly a factor of 6 greater than the total Borrelly production rate observed near the time of the DS1 encounter. We suggest that a likely explanation might be a strong asymmetry in the neutral coma caused by the large jets seen on the dayside of Borrelly. This would concentrate most of the gas

production rate into a smaller volume, creating the appearance locally of a higher total production rate.

There is no clear evidence in the TOF spectrum for mass/charge 28, which would appear as a shoulder in the water group peak. Further analysis will allow us to set an upper limit on the CO^+ abundance at Borrelly (since the TOF system is capable of separating CO^+ and N_2^+), and determine whether Borrelly is depleted in CO as well as C_2 and C_3 as indicated by ground-based observations (Fink et al., 1999; Szabó et al., 2002). Our initial analysis indicates the CO^+ abundance is under 10%, compared to 25% measured at Halley (Eberhardt et al., 1987). Finally, ions in the 12–15 AMU range are not resolved because they lie in the wings of the strong water group peaks. Extracting the abundance of these species and placing a better upper limit on the CO abundance will require detailed and accurate knowledge of the shapes of the molecular ion peaks. We are presently performing laboratory experiments to resolve this issue.

4. Conclusions

Initial analysis of PEPE observations reveals that Borrelly is very different in several ways from other comets visited by spacecraft. Perhaps the most prominent difference in the plasma environment is the global asymmetry of the entire solar wind interaction with Borrelly. The large collimated jets observed by the MICAS camera most likely have some effect on this displacement. Although the camera is primarily sensitive to emissions from dust (Soderblom et al., 2002), ground based telescopic observations suggest that Borrelly gas production is also very non-uniform and primarily sunward pointing (Weaver et al., 2003; Schleicher et al., 2003; Szabó et al., 2002). It is unclear without detailed modeling whether the tilt of the jets northward, in the direction of the offset of plasma boundaries reported here, is sufficient to account for the offset of plasma boundaries.

Another factor that must be included in our analysis is the solar wind magnetic field (at the time of this writing the DS1 magnetic field data are not yet available). However, based on observations at other comets, the field would have piled up in front of the cometopause boundary, further slowing the flow as magnetic pressure builds up. The magnetic field would also accentuate deflection of the solar wind to one side of the coma depending on the interplanetary field's spiral angle (Schmidt and Wegmann, 1991). Similarly, gyroradius effects can cause asymmetries near the nucleus (Luhmann et al., 1988) that depend on the strength and orientation of the magnetic field. However, the charge state of solar wind He^{2+} is primarily sensitive to the neutral density of the coma, while its speed is sensitive to the total ion pickup density. These both suggest that the 1000–2000 km northward offset observed by PEPE is a result of an asymmetric distribution of gas in the coma rather than magnetic field or gyroradius effects. The time dependence of gas production before closest approach, and the shape of the expansion during that period, may be other important factors.

Perhaps the most interesting aspect of the entire suite of DS1 data is that Borrelly presents a unique opportunity to track features in the plasma environment back to gas and possibly dust production and their dynamics. Although PEPE observations are confined to a single trajectory through the coma, it nonetheless may be possible to combine PEPE plasma data, ground observations of the neutral coma, and MICAS jet observations to model the distribution of plasma, neutral gas and dust in a self-consistent way. Such a model would for the first time give a complete view of cometary processes from the active geology of the nucleus' surface to conditions in the upstream solar wind.

Acknowledgments

We thank Southwest Research Institute (IR project 15.R9771) and Los Alamos National Laboratory/Department of Energy (WO-9165), which supported initial research and development of the PEPE instrument. We also express our thanks to many exceptional engineers and technicians at Southwest Research Institute, Los Alamos National Laboratory, and the Jet Propulsion Laboratory for their dedication to the development and operation of the PEPE instrument. We also thank S.P. Gary and M.F. Thomsen of Los Alamos for their support. PEPE development, operations, and (minimal) data analysis were supported by NASA and the Jet Propulsion Laboratory under contracts 960439, 960619, 961207 to Southwest Research Institute, Agreement #DE-FI04-00AL66167 with LANL, and 1216657 to the University of Michigan.

References

Balsiger, H., 1989. Measurements of ion species within the coma of Comet Halley from Giotto. In: Mason (Ed.), Comet Halley, Vol. 1, pp. 129–146.

Balsiger, H., 18 colleagues, 1986. Ion composition and dynamics at Comet Halley. Nature 321, 330–334.

Bame, S.J., Anderson, R.C., Asbridge, J.R., Baker, D.N., Feldman, W.C., Fuselier, S.A., Godling, J.T., McComas, D.J., Thomsen, M.F., Young, D.T., Zwickl, R.D., 1986. Comet Giacobini–Zinner—plasma description. Science 232, 356–361.

Coates, A.J., 12 colleagues, 1993. Pickup water group ions at Comet Grigg–Skjellerup. Geophys. Res. Lett. 20, 483–486.

Cravens, T.E., 1991. Plasma processes in the inner coma. In: Newburn, R.L., Neugebauer, M., Rahe, J. (Eds.), Comets in the Post-Halley Era. Kluwer Academic, Dordrecht, pp. 1211–1255.

Cravens, T.E., 1997. Comet Hyakutake *X*-ray source: charge transfer of solar wind heavy ions. Geophys. Res. Lett. 24, 105–108.

Cravens, T.E., 2002. X-ray emission from comets. Science 296, 1042–1045.

Eberhardt, P., Krankowsky, D., Schulte, W., Dolder, U., Lammerzahl, P., Berthelier, J.J., Woweries, J., Stubbemann, U., Hodges, R.R., Hoffman, J.H., Illiano, J.M., 1987. The CO and N_2 abundance in Comet P/Halley. Astron. Astrophys. 187, 481.

Fink, U., Hicks, M.P., Fevig, R.A., 1999. Production rates in the Stardust mission target: 81P/Wild 2. Icarus 141, 331–340.

Funsten, H.O., McComas, D.J., Barraclough, B.L., 1993. Ultrathin foils used for low energy neutral atom imaging of planetary magnetospheres. Optical Eng. 32, 3090–3095.

Gary, S.P., Hinata, S., Madland, C.D., Winske, D., 1986. The development of shell like distributions from newborn cometary ions. Geophys. Res. Lett. 13, 1364–1367.

Greenwood, J.B., Chutjian, A., Smith, S.J., 2000. Measurements of absolute, single charge-exchange cross sections of H^+, He^+, and He^{++} with H_2O and CO_2. Astrophys. J. 529, 605–609.

Gombosi, T.I., 1987. Charge-exchange avalanche at the cometopause. Geophys. Res. Lett. 14, 1174–1177.

Haberli, R.M., Altwegg, K., Balsiger, H., Geiss, J., 1995. Physics and chemistry of ions in the pile-up region of Comet P/Halley. Astron. Astrophys. 297, 881.

Haberli, R.M., Combi, M.R., Gombosi, T.I., DeZeeuw, D.L., Powell, K.G., 1997. Quantitative analysis of H_2O^+ coma images using a multiscale MHD model with detailed ion chemistry. Icarus 130, 373–386.

Haser, L., 1957. Distribution d'intensité dans la têd' une comète. Bull. Acad. Roy. Belgique Class. Sci. 43, 740–750.

Huddleston, D.E., Neugebauer, M., Goldstein, B.E., 1994. Modeling of pickup ion distributions in the Halley cometosheath—empirical limits on rates of ionization, diffusion, loss and creation of fast neutral atoms. J. Geophys. Res. 99, 19245–19254.

Huebner, W.F., Boice, D.C., Schmidt, H.U., Wegmann, R., 1991. Structure of the coma: chemistry and solar wind interaction. In: Newburn, R.L., Neugebauer, M., Rahe, J. (Eds.), Comets in the Post-Halley Era, Vol. 2. Kluwer Academic, Dordrecht, pp. 907–935.

Ip, W.-H., 1988. Cometary ion-acceleration processes. Comput. Phys. Commun. 49, 1–7.

Ip, W.-H., Axford, W.I., 1990. 5. The plasma. In: Heubner, W.F. (Ed.), Physics and Chemistry of Comets. Springer-Verlag, Berlin, pp. 177–233.

Ipavich, F.M., Galvin, A.B., Gloeckler, G., Hovestadt, D., Klecker, B., Scholer, M., 1986. In situ observations of energetic heavy ions. Science 232, 366–369.

Johnstone, A., 27 colleagues, 1986. Ion flow at Comet Halley. Nature 321, 344–347.

Johnstone, A.D., Huddleston, D.E., Coates, A.J., 1991. The spectrum and energy density of solar wind turbulence of cometary origin. In: Johnstone, A.D. (Ed.), Cometary Plasma Processes. In: AGU Monogr. Ser., Vol. 61. American Geophysical Union, Washington, DC, pp. 259–272.

Johnstone, A., Coates, A.J., Huddleston, D.E., Jockers, K., Wilken, B., Borg, H., Gurgiolo, C., Winningham, J.D., Amata, E., 1993. Observations of the solar wind and cometary ions during the encounter between Giotto and P/Grigg–Skjellerup. Astron. Astrophys. 273, L1–L4.

Klummer, K.R., 1991. The global interaction of comets with the solar wind. In: Newburn, R.L., Neugebauer, M., Rahe, J. (Eds.), Comets in the Post-Halley Era, Vol. 2. Kluwer Academic, Dordrecht, pp. 1125–1141.

Krankowsky, D., 11 colleagues, 1986. In situ gas and ion measurements at Comet Halley. Nature 321, 326–329.

Luhmann, J.G., Fedder, J.A., Winske, D., 1988. A test particle model of pickup ions at Comet Halley. J. Geophys. Res. 93, 7532–7537.

McComas, D.J., Nordholt, J.E., 1990. A new approach to 3-D, high sensitivity, high mass resolution space plasma composition measurements. Rev. Sci. Inst. 61, 3095–3097.

McComas, D.J., Nordholt, J.E., Young, D.T., Berthelier, J.J., 1998. The Cassini mass spectrometer. In: Pfaff, R.F., Borovsky, J.E., Young, D.T. (Eds.), Measurement Techniques in Space Plasmas: Particles. In: AGU Monogr. Ser., Vol. 102. American Geophysical Union, Washington, DC, pp. 187–193.

Mendis, D.A., Smith, E.J., Tsurutani, B.T., Slavin, J.A., Jones, D.E., Siscoe, G.L., 1986. Comet–solar wind interactions—dynamic length scales and models. Geophys. Res. Lett. 13, 239–242.

Neubauer, F.M., 1991. The magnetic field structure of the cometary plasma environment. In: Newburn, R.L., Neugebauer, M., Rahe, J. (Eds.), Comets in the Post-Halley Era, Vol. 2. Kluwer Academic, Dordrecht, pp. 1107–1124.

Rayman, M.D., 2002. The Deep Space 1 extended mission: challenges in preparing for an encounter with Comet Borrelly. Acta Astron. 51, 507–516.

Reme, H., 1991. Cometary plasma observations between the shock and the contact surface. In: Johnstone, A.D. (Ed.), Cometary Plasma Processes. AGU Monogr. Ser., Vol. 61. American Geophysical Union, Washington, DC, pp. 87–106.

Sauer, K., Bogdanov, A., Baumgartel, K., 1994. Evidence of an ion composition boundary (protonopause) in bi-ion fluid simulations. Geophys. Res. Lett. 21, 2255–2258.

Schmidt, H.U., Wegmann, R., 1991. An MHD model of cometary plasma and comparison with observations. In: Johnstone, A.D. (Ed.), Cometary Plasma Processes. In: AGU Monogr. Ser., Vol. 61. American Geophysical Union, Washington, DC, pp. 49–63.

Schleicher, D.G., Woodney, L.M., Millis, R.L., 2003. Comet 19P/Borrelly at multiple apparitions: seasonal variations in gas production and dust morphology. Icarus 162, 415–442.

Schmidt, H.U., Wegmann, R., Neubauer, F.M., 1993. MHD modeling applied to Giotto encounter with Comet P/Grigg–Skjellerup. J. Geophys. Res. 98, 21009–21016.

Sekanina, Z., 1991. Cometary activity, discrete outgassing areas, and dust-jet formation. In: Newburn, R.L., Neugebauer, M., Rahe, J. (Eds.), Comets in the Post-Halley Era, Vol. 2. Kluwer Academic, Dordrecht, pp. 769–824.

Shelley, E.G., Fuselier, S.A., Balsiger, H., Drake, J.F., Geiss, J., Goldstein, B.E., Goldstein, R., Ip, W.-H., Lazarus, A.J., Neubauer, F.M., 1987. Charge-exchange of solar-wind ions in the coma of Comet P/Halley. Astron. Astrophys. 187, 304–306.

Soderblom, L.A., 21 colleagues, 2002. Observations of Comet 19P/Borrelly by the miniature integrated camera and spectrometer aboard Deep Space 1. Science 296, 1087–1091.

Szabó, Gy.M., Kiss, L.L., Sárnecky, K., Sziládi, K., 2002. Spectrophometry and structural analysis of 5 comets. Astron. Astrophys. 382, 702–710.

Thomsen, M.F., Bame, S.J., Feldman, W.C., Gosling, J.T., McComas, D.J., Young, D.T., 1986. The comet/solar wind transition region at Giacobini–Zinner. Geophys. Res. Lett. 13, 393–396.

Tsurutani, B.T., Glassmeier, K.H., Neubauer, F.M., 1995. An intercomparison of plasma turbulence at 3 comets—Grigg–Skjellerup, Giacobini–Zinner, and Halley. Geophys. Res. Lett. 22, 1149–1152.

Tsurutani, B.T., 1991. Cometary plasma waves and instabilities. In: Newburn, R.L., Neugebauer, M., Rahe, J. (Eds.), Comets in the Post-Halley Era, Vol. 2. Kluwer Academic, Dordrecht, pp. 1171–1210.

Weaver, H.A., Stern, S.A., Parker, J.Wm., 2003. Hubble Space Telescope STIS observations of Comet 19P/Borrelly during the Deep Space 1 encounter. Astron. J. 126, 444–451.

Yoon, P.H., Wu, C.S., 1991. Ion pickup in the solar wind via wave-particle interaction. In: Johnstone, A.D. (Ed.), Cometary Plasma Processes. In: AGU Monogr. Ser., Vol. 61. American Geophysical Union, Washington, DC, pp. 241–258.

Young, D.T., 27 colleagues, 2003. Plasma experiment for planetary exploration (PEPE). Space Sci. Rev. Submitted for publication.